MIT Open Access Articles

Thrust Inference for Ionic-Liquid Electrospray Thrusters on a Magnetically-Levitating Thrust Balance

Thrust Inference for Ionic-Liquid Electrospray Thrusters on a Magnetically-Levitating Thrust Balance

IEPC-2022-208

Oliver Jia-Richards[1], Matthew N. Corrado[2], and Paulo C. Lozano[3]
Massachusetts Institute of Technology, Cambridge, MA, USA

Magnetically-levitating thrust balances offer advantages over traditional pendulum-based thrust stands due to their physical and electrical isolation from their environments, enabling increased accuracy and stability resulting from decreased measurement noise and long-term drift. In addition, magnetically-levitated balances can operate with at least one unconstrained and friction-free degree of freedom, increasing their sensitivity as even vanishingly small forces can be detected over firing periods long enough for the time-dependent displacement to be resolved. However, there are two key challenges associated with thrust inference on a magnetically-levitating balance. The first is quantification of uncertainty in the thrust output caused by measurement noise or uncertainty in the test setup. The second is differentiating the thrust output when a pair of thrusters is used in order to maintain charge neutrality. This paper presents a method for resolving both of these key challenges. The method is then applied to experimental data in order to demonstrate the ability to perform thrust inference on a pair of thrusters on a magnetically-levitating thrust balance. The mean values of the inferred thrust outputs are consistent with prior methods that only determined the average combined thrust output of the thruster pair, and the 3σ uncertainty of the thrust outputs is approximately 10%.

I. Introduction

Measurement of thrust is one of the most critical aspects of characterizing space propulsion devices. Interest in increasingly small propulsion systems has introduced new challenges related to directly and accurately measuring thrust at the micro-Newton level, and has necessitated the development of more sensitive instruments to properly characterize microthrusters in a laboratory setting. Most commonly, thrust from electric propulsion systems is inferred using the motion of pendulum-based thrust stands [1]. However, pendulum thrust stands carry many disadvantages, one of which is their limited precision due to noise that is introduced as a result of the thrust stand being fixed to its environment. Alternative instruments have been developed to isolate the thrust stand from its environment in order to decrease the influence of random errors on thrust measurements. One such instrument is a magnetically-levitating thrust balance where a test vehicle is magnetically levitated in order to provide one friction-less rotational degree of freedom [2]. Thrusters can then be used to produce torques on the test vehicle, and by measuring the resulting change in rotation of the test vehicle the thrust can be inferred [3].

A magnetically-levitating thrust balance has been demonstrated to provide consistent thrust measurements for a pair of ionic-liquid electrospray thrusters relative to traditional thrust stands [4]. However, there are two key challenges for characterizing the thrust output of electrospray thrusters with a magnetically-levitating thrust balance. The first is proper quantification of uncertainty in the thrust measurement. Uncertainty can be produced from a variety of sources such as measurement noise as well as uncertainty in the test setup itself, including the rotational inertia of the test vehicle or the lever arm of the thrusters. Prior approaches typically attempt to bound this uncertainty by taking a large sample of measurements at equivalent conditions and using the variance of the data set as an indicator of random uncertainty [3].

---

[1]Doctoral Candidate, Department of Aeronautics and Astronautics
[2]Doctoral Candidate, Department of Aeronautics and Astronautics
[3]Miguel Alemán-Velasco Professor, Department of Aeronautics and Astronautics
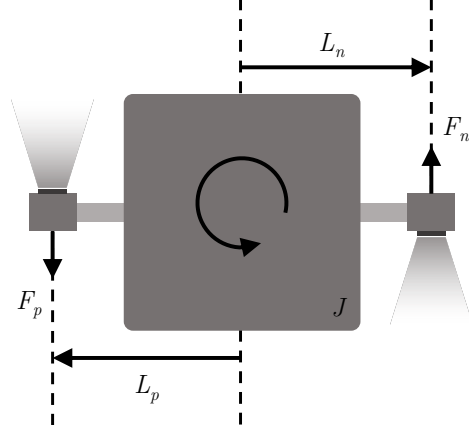
Fig. 1   Notional diagram of the magnetically-levitating thrust balance setup.

However, limitations to this approach include the inability to ensure identical conditions between data points due to drift in thruster output as well as difficulty in incorporating uncertainty in the test setup. In addition, the contact-free requirement of the magnetically-levitated thrust stand makes it challenging to calibrate it against systematic errors using known forces, a technique commonly used with pendulum thrust stands [1].

The second challenge is driven by the need to avoid significant electrical charging of the test vehicle. Due to the contact-free requirement of the thrust balance, the test vehicle cannot be grounded to the chamber itself in order to avoid charge buildup on the vehicle. Instead, typical operation involves the use of a pair of electrospray thrusters; one thruster emits positively-charged ions while the other thruster emits negatively-charged ions. By constraining the thrusters to emit equal magnitudes of current, charging of the test vehicle can be mitigated [5]. While using a pair of thrusters resolves the vehicle charging problem, it confounds the thrust inference as the thrust output of the individual thrusters cannot be determined based on a single measurement of the torque acting on the test vehicle. This limitation means that prior results for the thrust output measured on a magnetically-levitating thrust balance report the total thrust output of an electrospray thruster pair rather than the thrust output of individual thrusters [3, 4].

This paper aims to address both of the identified key challenges for measuring thrust on a magnetically-levitating thrust balance. Inherent differences in the performance of the thrusters in a thruster pair can be leveraged in order to differentiate their thrusts by taking torque measurements at multiple operating points. Furthermore, the use of numerical Bayesian inference techniques such as the ensemble Kalman update allows for the uncertainty in the thrust output to be directly quantified in the presence of both measurement and test setup uncertainty. Resolving both of these key challenges will enable direct thrust measurements on a magnetically-levitating thrust balance to be performed in a rigorous manner, and allow for comparison to measurements taken on traditional thrust balances [6, 7] as well as indirect thrust measurement techniques [8, 9]. Section II introduces the approach for differentiating the thrust outputs of the individual thrusters in a thruster pair while Section III outlines the implementation for performing thrust inference based on data collected on a magnetically-levitating thrust balance. Section IV demonstrates the efficacy of the overall approach on simulated data. Finally, Section V utilizes the developed approach in order to experimentally characterize the thrust output of a pair of ionic-liquid electrospray thrusters.

II. Approach

Figure 1 shows a notional diagram of the magnetically-levitating thrust balance setup. A bipolar pair of electrospray thrusters is mounted on a test vehicle with rotational inertia J. The thrust produced by the positive-polarity thruster has a thrust magnitude of F_p and a lever arm of L_p with respect to the test vehicle's center of mass. Similarly, the negative-polarity thruster has a thrust magnitude of F_n and lever arm of L_n. When operated, the pair of thrusters produces a torque on the test vehicle that will cause it to rotate. In this work it is assumed that the thrust vectors of each thruster are aligned such that the torque they produce on the test vehicle is aligned with the test vehicle's axis of rotation. Although misalignment in thruster mounting as well as off-axis emission from the thruster would cause misalignment between the torque vector and the axis of rotation, these effects cannot be characterized in the current test setup.

Theoretical analysis as well as experimental evidence shows that the thrust of an electrospray thruster operating in

the pure-ion regime is well characterized by

$$F = \phi I \sqrt{V} \tag{1}$$

where F is the thrust output, ϕ is the thrust coefficient, I is the emitted current, and V is the thruster potential [6, 7, 10]. The total torque produced by the pair of thrusters on the test vehicle is then

$$\tau = I \left[\phi_p L_p \sqrt{V_p} + \phi_n L_n \sqrt{V_n} \right] \tag{2}$$

where I is the emitted current of each thruster, $V_{p/n}$ are the thruster potentials required for the positive-polarity and negative-polarity thrusters to produce current I respectively, and $\phi_{p/n}$ are the thrust coefficients for the positive-polarity and negative-polarity thrusters. As mentioned previously, the magnitude of the current outputs of the positive-polarity and negative-polarity thrusters need to be equal for steady-state charging of the test vehicle to be achieved.

The magnetically-levitating thrust balance allows for the total torque produced by the pair of thrusters to be observed by measuring the change in the test vehicle's angular position over time. If the current output and thruster potential for each thruster can also be measured during testing, then the only remaining unknown is the thrust coefficient. Instead of attempting to directly estimate the thrust output of each thruster—as is typically done during laboratory thrust characterization—the goal of this work is to estimate the thrust coefficients. The key idea is that if the pair of thrusters is operated at two different current levels, then a linear system relating the desired thrust coefficients to the observed torques can be defined

$$\begin{bmatrix} \tau_1 \\ \tau_2 \end{bmatrix} = \begin{bmatrix} I_1 & 0 \\ 0 & I_2 \end{bmatrix} \begin{bmatrix} \sqrt{V_{p,1}} & \sqrt{V_{n,1}} \\ \sqrt{V_{p,2}} & \sqrt{V_{n,2}} \end{bmatrix} \begin{bmatrix} L_p & 0 \\ 0 & L_n \end{bmatrix} \begin{bmatrix} \phi_p \\ \phi_n \end{bmatrix} \tag{3}$$

where τ_1 is the torque measured at current I_1, τ_2 is the torque measured at current I_2, $V_{p,i}$ is the thruster potential required for the positive-polarity thruster to produce current I_i, and $V_{n,i}$ is the thruster potential required for the negative-polarity thruster to produce current I_i. As long as $I_1 \neq 0$, $I_2 \neq 0$, $L_p \neq 0$, $L_n \neq 0$, and

$$\det \begin{bmatrix} \sqrt{V_{p,1}} & \sqrt{V_{n,1}} \\ \sqrt{V_{p,2}} & \sqrt{V_{n,2}} \end{bmatrix} \neq 0 \tag{4}$$

then a unique mapping exists between the torques and the thrust coefficients, allowing the thrust coefficients of each thruster to be determined. The condition of Eq. 4 will be met if

$$\frac{V_{p,1}}{V_{p,2}} \neq \frac{V_{n,1}}{V_{n,2}} \tag{5}$$

which simply means that the factor by which the thruster potential scales when the current changes from I_1 to I_2 must be different for the two thrusters.

Since the thruster potential drives the thruster's output current, the two thrusters having different current-voltage relationships is a necessary condition for Eq. 5. Although in theory different current-voltage relationships is not a sufficient condition for Eq. 5, in practice different current voltage relationships will likely imply that Eq. 5 is met. Differences in the current-voltage relationships between the two thrusters can be caused by operating in opposite polarities as well as manufacturing and assembly differences. While differences in the manufacturing and assembly of thrusters is typically undesired, they can be used here in order to allow the thrust coefficients of multiple thrusters to be differentiated. In this work, only a pair of bipolar thrusters is being considered. However, this same approach can be applied to an arrays with an arbitrary number of thrusters; for an array of m thrusters, m different current levels will be required, and all m thrusters will need to have different current-voltage relationships.

III. Implementation

The analysis of Section II suggests that by operating the pair of thrusters at two different current levels, the individual thrust coefficient for each thruster can be determined. In order to actually translate the measured angular position of the test vehicle into individual thrust coefficients, an inference problem is defined. Specifically, for k measurement times, the measurement vector is

$$y = \begin{bmatrix} \theta(t_1) & \theta(t_2) & \dots & \theta(t_k) \end{bmatrix}^T \tag{6}$$

where $\theta(t_i)$ is the measured angular position of the test vehicle at measurement time i. Given a particular measurement vector, the goal is to infer a parameter vector

$$\phi = \begin{bmatrix} \theta_0 & \omega_0 & \phi_p & \phi_n \end{bmatrix} \tag{7}$$

where θ_0 and ω_0 are the initial angular position and velocity of the test vehicle respectively. In order to solve the inference problem, an ensemble Kalman update is used [11], which provides an ensemble of estimates for the parameter vector based on an observed measurement vector.

The core component of the ensemble Kalman update is a model that simulates measurement vectors for assumed parameter vectors. For this problem, the model is a propagation of the test vehicle's angular position over time for a given initial angular position and velocity as well as assumed thrust coefficients for each thruster. The torque acting on the test vehicle at any instant in time is calculated according to Eq. 2. In order to account for the requirement that two different current levels be used, for a given overall simulation time it is assumed that the thrusters are operated at current level I_1 for the first half of the simulation time and then operated at current level I_2 for the second half. The model also includes measurement noise, which for this test setup was experimentally measured to be normally distributed with standard deviation of 1.3 degrees.

A final aspect of the model is accounting for uncertainty in the test setup. The rotational inertia of the test vehicle as well as the lever arms of each thruster are uncertain, and that uncertainty will induce uncertainty in the estimated thrust coefficients. The rotational inertia of the test vehicle can be measured with a trifilar pendulum, and for this particular test setup the uncertainty in the rotational inertia is normally distributed with mean value of 6.17 gm^2 and 3σ uncertainty of 0.0329 gm^2. The lever arm of each thruster can be separated into two components

$$L_{p/n} = l_{p/n} + c_{p/n} \tag{8}$$

where l corresponds to the distance between the test vehicle's center of mass and the geometric center of the thruster and c corresponds to the offset in the thruster's center of thrust relative to the thruster's geometric center. Uncertainty in the measurement of the distance between the test vehicle's center of mass and the geometric center of the thruster is assumed to be uniformly distributed with mean value of 13.25 cm and interval length of 0.5 mm.

Uncertainty in the offset in the thruster's center of thrust relative to the thruster's geometric center is more difficult to quantify. Emission of current across an electrospray array is known to be non-uniform [12–14], and this non-uniformity is what will cause the offset between the center of thrust and geometric center. Detailed quantification of the spatial non-uniformity of emission has yet to be conducted. As such, the offset between the center of thrust and geometric center is assumed here to be uniformly distributed with an interval length of 40% the overall thruster dimension. Since the thrusters used in this work are square with side lengths of approximately 10 mm, the center of thrust is assumed to be within ±2 mm of the thruster's geometric center. This selection of distribution for the offset between the center of thrust and geometric center is arbitrary, and will need to be updated when the spatial non-uniformity of emission across an electrospray array has been characterized quantitatively.

The uncertainty in the test setup can be accounted for in the model by assigning a random rotational inertia and thruster lever arms to each ensemble member based on the assumed distributions. The forward model is then stochastic, and simulates both noise caused by measurement noise as well as noise in the test vehicle's angular position caused by model uncertainty. When used in the ensemble Kalman update, the distribution of parameter vectors for the ensemble members allows for quantification of uncertainty in the parameters of inference, and accounts for uncertainty due to modeling error. The combination of using the ensemble Kalman update with model uncertainty along with operating the pair of thrusters at two different current levels allows for both key challenges to be solved; separate thrust coefficients for each thruster will be determined—differentiating the thrust outputs of each thruster—and the uncertainty in those thrust coefficients will be quantified based on the posterior distribution of the parameter vectors in the ensemble.

IV. Simulated Results

In order to demonstrate the efficacy of the overall approach and implementation, simulated tests were conducted where the true thrust coefficients of each thruster are known. Figure 2 shows an experimentally-obtained current-voltage relationship for a single electrospray thruster in both the positive and negative polarities. For this test case, it is assumed that one thruster is operating in the positive polarity and uses the positive current-voltage relationship in Figure 2 while the other thruster is operating in the negative polarity and uses the negative current-voltage relationship in Figure 2. As the same thruster was used to obtain both the positive-polarity and negative-polarity current-voltage relationships,
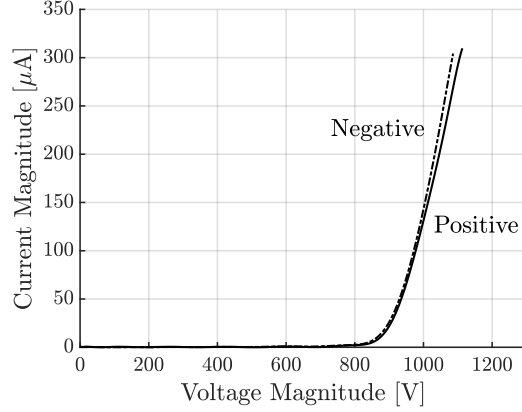
Fig. 2   Current-voltage curve in both the positive and negative polarities for a single thruster.
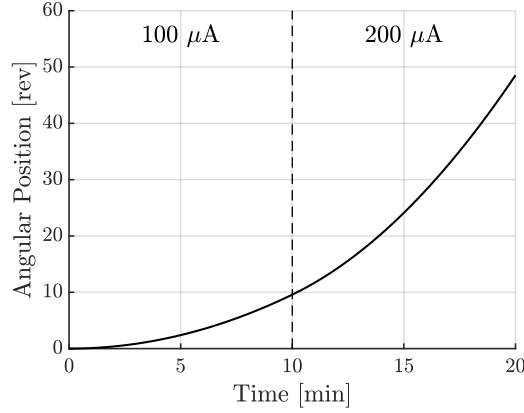

Fig. 3   Simulated angular position over time.

the only differences between the relationships are caused by the difference in polarities, and no differences caused by manufacturing and assembly are present. Therefore, this test case is relatively challenging as the current-voltage curves for either polarity are quite similar, which will make it more difficult to determine the individual thruster coefficients.

The true thrust coefficients were chosen to be ϕ_p = 2 mN/A$\sqrt{V}$ and ϕ_n = 3 mN/A$\sqrt{V}$. For the simulation, the thrusters were first operated at 100 μA for 10 minutes and then operated at 200 μA for a further 10 minutes. Measurements were assumed to be taken at an interval of 1 s. Figure 3 shows the simulated angular position of the test vehicle over time assuming the test vehicle is initially at rest. Based on the current-voltage relationships of Figure 2, the positive-polarity thruster required thruster potentials of 977 V and 1046 V in order to produce 100 μA and 200 μA respectively, while the negative-polarity thruster required thruster potentials of 972 V and 1033 V. The ratio in thruster potentials is then $V_{p,1}/V_{p,2}$ = 0.934 for the positive-polarity thruster and $V_{n,1}/V_{n,2}$ = 0.941 for the negative-polarity thruster. While these ratios are quite similar, they are different. Therefore, the condition of Eq. 5 is met and it should be possible to determine the individual thrust coefficients of each thruster.

Figure 4 shows the marginal posterior distributions of the errors in the thrust coefficient estimates based on the ensemble of parameter estimates returned by the ensemble Kalman update with 10^4 ensemble members. The inferred mean values for ϕ_p and ϕ_n were 2.11 mN/A$\sqrt{V}$ and 2.88 mN/A$\sqrt{V}$ respectively. Both values had 3σ uncertainties of 0.57 mN/A$\sqrt{V}$, or approximately 23% of the true values. Figure 5 shows a scatter plot of the errors in the thrust coefficient estimates from the posterior ensemble, and shows a significant correlation between estimates of ϕ_p and ϕ_n with a Pearson correlation coefficient of -0.96. Much of the posterior uncertainty in the thrust coefficients as well as the high correlation is caused by there only being a slight difference in the current-voltage relationships between the two thrusters. If the thruster potential required for the positive-polarity thruster to produce 200 μA is only slightly increased
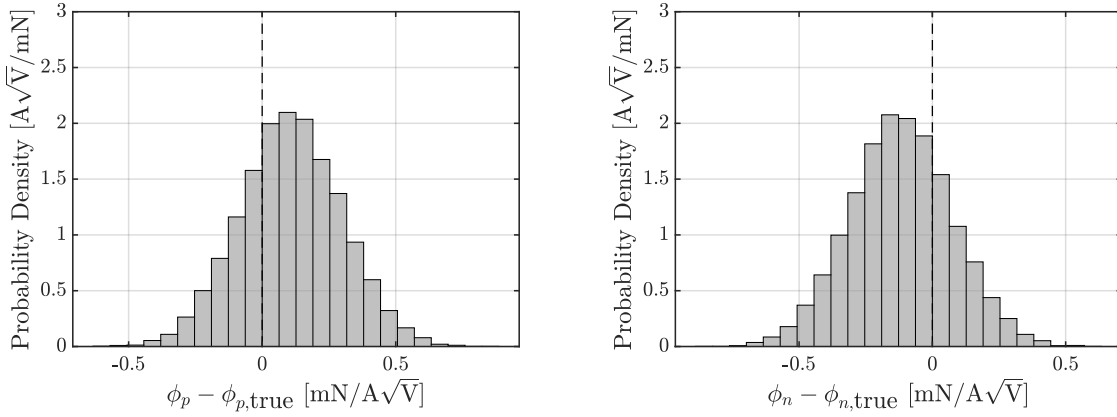
5

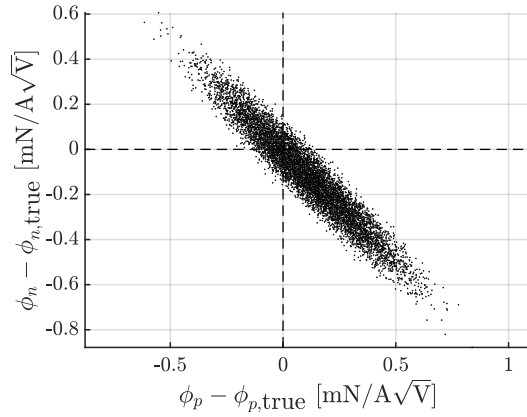**Fig. 4 Posterior distributions of the inferred thrust coefficient errors from simulated data.**

Fig. 5 Scatter plot of the inferred thrust coefficient error from simulated data.

by 1% to 1057 V, then the 3σ uncertainty in the thrust coefficients is reduced by over a factor of two to 0.26 mN/A$\sqrt{V}$, approximately 10% of the true values, and the Pearson correlation coefficient is -0.80, indicating better differentiation between the thrust coefficients of the two thrusters.

V. Experimental Results

Thrust experiments were conducted with a pair of laboratory electrospray thrusters using the ionic liquid 1-ethyl-3-methylimidazolium tetrafluoroborate (EMI-BF$_4$) as propellant [4]. Commanding of the thruster potential and recording of the applied potential and emitted currents is managed through a remote-controlled power processing unit [2]. All experiments were conducted in a 2.8 m^3 vacuum chamber equipped with two cryogenic pumps with a total pumping capacity of 7,000 L/s of xenon. The chamber pressure remained below 5×10^{-6} Torr throughout all experiments. Any lateral motion of the test satellite caused by the cryogenic pumps is damped over time using magnetic dampers, resulting in pure rotation of the satellite about its central axis prior to the start of any experiments.

The thrusters' emitters are electrically connected in a series configuration, with the high- and low-voltage circuits separated using galvanic isolation. Such a configuration constrains the thrusters to always emit equal and opposite currents, ensuring that significant electrical charging of the satellite is avoided. When the thrusters are commanded to fire, a command is sent to the power processing unit, which applies equal and opposite high voltage to the thrusters. However, if the current-voltage characteristics of the two thrusters are not symmetric and identical, they will tend to emit different current magnitudes at equal emitter biases. Since a physical constraint prevents differences in current magnitudes, the actual potential difference experienced by one of the two thrusters may be different than the commanded
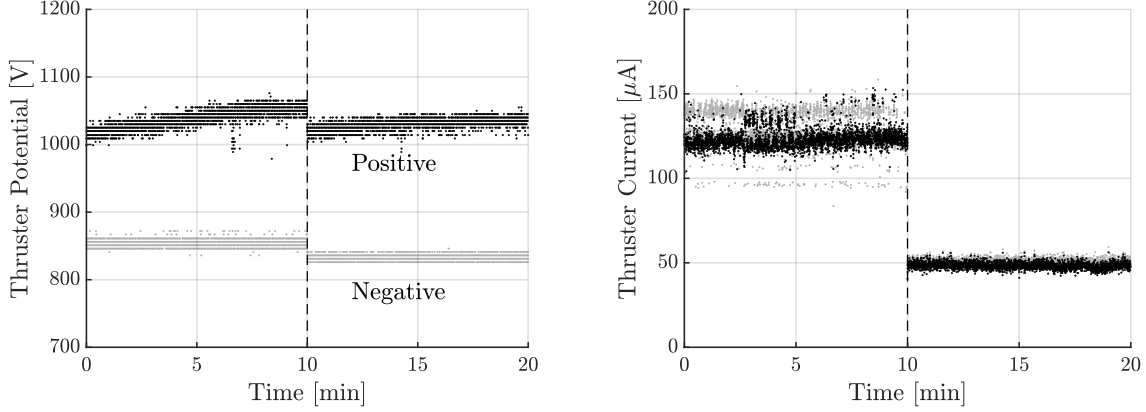
Fig. 6 Measured magnitude of the thruster potentials and emitted currents.

voltage to satisfy the constraint. For the same reasons, the maximum current achievable by the pair is limited by the thruster with the shallower current-voltage curve.

Thrust measurements were performed by using the same pair of thrusters at two distinct current levels, 150 μA and 50 μA. The potential difference and emitted currents for both thrusters were continuously measured by the power processing unit. Angular position was measured using a webcam-based optical sensor mounted underneath the levitated satellite. Without making physical contact, the webcam views and records a fiducial pattern printed on the bottom face of the satellite, and software is used to interpret the pattern and calculate the angular position relative to an arbitrary zero [2]. Prior to performing thrust measurements, the thrusters were conditioned by firing in both polarities for several minutes to mitigate long-term transients associated with fluid dynamics.

Once the thrusters were operating at near-steady state, measurements were performed by first bringing the test satellite to rest using electromagnetic brakes and commanding the thrusters to fire, first at 150 μA for 10 minutes and subsequently at 50 μA for another 10 minutes. The firing potential was modulated via closed-loop control in order to maintain constant current. Figure 6 shows the measured magnitude of the thruster potentials and emitted currents throughout the experiment. Note that the thruster potential for the positive-polarity thruster slightly changes over time—likely due to insufficient conditioning. This change in the thruster potential is accounted for during post-processing of the experimental data in order to determine the thrust coefficients. Also note that the emitted thruster currents are lower than the commanded 150 μA due to a significant fraction of the current being intercepted by the thrusters' extractor grids and therefore not being emitted out of the thruster. The apparent separation in current levels during the first ten minutes is caused by flickering in the current output of the negative-polarity thruster; both thrusters maintained an average emitted current of approximately 126 μA during the first ten minutes. The ratios of mean values of the thruster potentials were $V_{p,1}/V_{p,2} \approx 1.01$ and $V_{n,1}/V_{n,2} \approx 1.03$ indicating that the condition of Eq. 5 is met.

Figure 7 shows the measured angular position of the test satellite over time and Figure 8 shows the inferred distributions of the thrust coefficients. The inferred mean values for the thrust coefficients were 3.33 mN/A$\sqrt{V}$ and 2.52 mN/A$\sqrt{V}$ for the positive- and negative-polarity thrusters respectively. Both values had 3σ uncertainties of approximately 0.28 mN/A$\sqrt{V}$, or approximately 10% of the inferred values. Figure 9 shows a scatter plot of the inferred thrust coefficient estimates. The Pearson correlation coefficient between the thrust coefficient estimates was -0.83. Given the estimated thrust coefficients, the thrust outputs of the thrusters during the experiment can be estimated from Eq. 1 given the measured thruster potentials and emitted currents. Figure 10 shows the estimated thrust output of the individual thrusters as well as the combined thrust output of the thruster pair. The grey dash-dot line for the combined thrust output shows the output of the prior method, outlined in Ref. [2], where only an average value for the combined thrust output of the thruster pair could be determined. The method of this paper is consistent with the prior method in predicting the average thrust output of the thruster pair, but also allows for the thrust outputs of the individual thrusters to be determined.
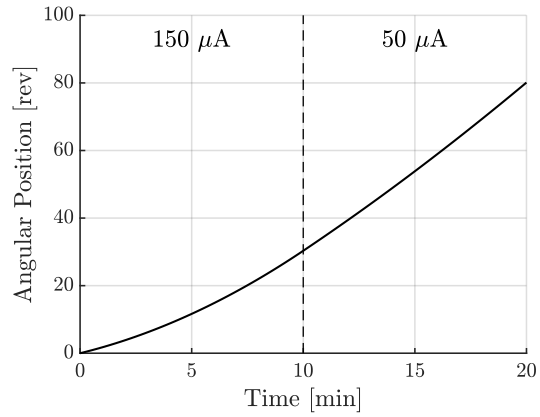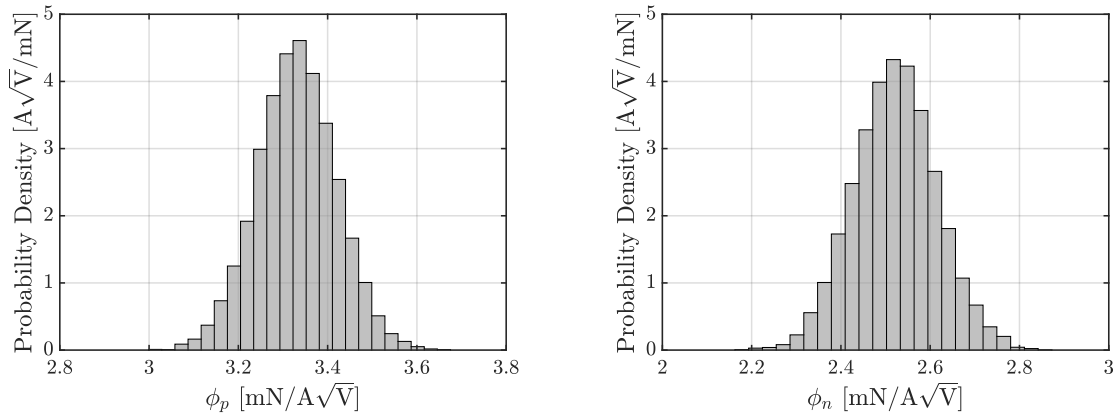
Fig. 7   Measured angular position over time.

Fig. 8   Posterior distributions of the inferred thrust coefficient errors from experimental data.
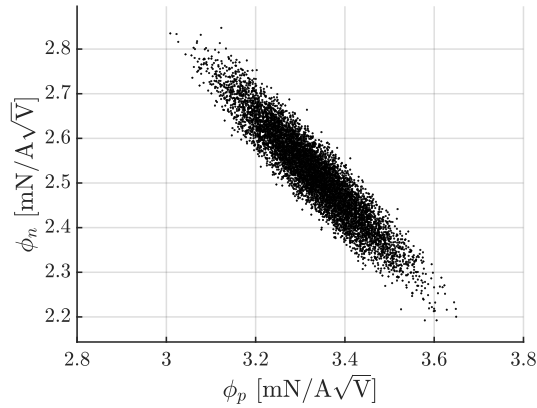

Fig. 9   Scatter plot of the inferred thrust coefficient error from experimental data.
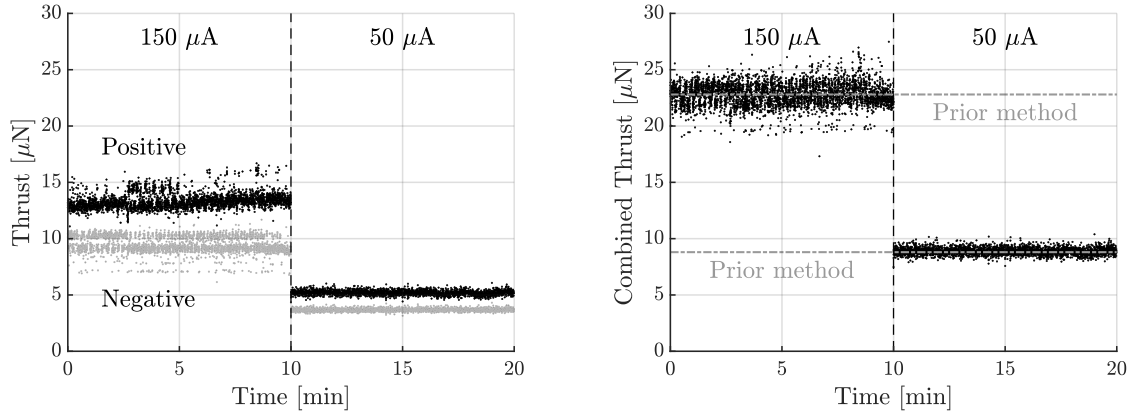
Fig. 10   Inferred thrust output of the individual thrusters (left) and combined thrust output of the thruster pair (right). Dash-dot lines show the prediction of the combined thrust output using the prior method.

VI. Conclusion

This paper resolves two key challenges for performing thrust inference of a pair of electrospray thrusters on a magnetically-levitating thrust balance. By leveraging inherent differences in the performance of electrospray thrusters as well as numerical inference techniques such as the ensemble Kalman update, the thrust output of the individual thrusters can be differentiated and the uncertainty in the thrust output can be quantified. Experimental results demonstrate the ability to determine the thrust coefficient for individual thrusters with 3σ uncertainty of approximately 10%. Since the uncertainty is tied to the thrust coefficient, the uncertainty in the thrust output at any specific thrust level will also have a 3σ value of 10%. The individual thrust values determined in this work are consistent with prior thrust measurements of similar thrusters taken with a traditional torsional balance [4].

While the method of this work was developed under the context of a bipolar pair of electrospray thrusters, the method can be applied for an arbitrary number of electrospray thrusters. Many proposed electrospray thruster systems feature arrays of multiple thrusters in order to scale the total thrust output of an electrospray-thruster-based propulsion system [8, 15–17]. Methods for on-orbit thrust inference are only capable of determining the overall combined thrust output of the propulsion system [18]. An approach similar to the one developed in this work could be used in order to differentiate the thrust output of each thruster on the array. The ability to determine individual thrust outputs would allow the performance of each thruster or the array to be characterized, and could provide insight into long-term trends in the performance of electrospray thrusters when integrated into large arrays.

Acknowledgements

References

[1] Polk, J. E., Pancotti, A., Haag, T., King, S., Walker, M., Blakely, J., and Ziemer, J., "Recommended Practices in Thrust Measurements," *33rd International Electric Propulsion Conference*, Washington DC, USA, 2013.

[2] Mier Hicks, F., "Spacecraft Charging and Attitude Control Characterization of Electrospray Thrusters on a Magnetically Levitated Testbed," Ph.D. thesis, Massachusetts Institute of Technology, 2017.

[3] Mier Hicks, F., and Lozano, P. C., "Thrust Measurements of Ion Electrospray Thrusters using a CubeSat Compatible Magnetically Levitated Thrust Balance," *34th International Electric Propulsion Conference*, Hyogo-Kobe, Japan, 2015.

[4] Krejci, D., Mier Hicks, F., Thomas, R., Haag, T., and Lozano, P. C., "Emission Characteristics of Passively Fed Electrospray Microthrusters with Propellant Reservoirs," *Journal of Spacecraft and Rockets*, Vol. 54, No. 2, 2017, pp. 447–458. https://doi.org/10.2514/1.A33531.

[5] Mier Hicks, F., and Lozano, P. C., "Spacecraft-Charging Characteristics Induced by the Operation of Electrospray Thrusters," *Journal of Propulsion and Power*, Vol. 33, No. 2, 2017, pp. 456–467. https://doi.org/10.2514/1.B36292.

[6] Fedkiw, T., Wood, Z., Demmons, N., and Courtney, D., "Environmental and Lifetime Testing of the BET-300-P Electrospray Thruster," *AIAA Propulsion and Energy Forum*, Virtual Event, 2020. https://doi.org/10.2514/6.2020-3614.

[7] Courtney, D. G., Dandavino, S., and Shea, H., "Comparing Direct and Indirect Thrust measurements from Passively Fed Ionic Electrospray Thrusters," *Journal of Propulsion and Power*, Vol. 32, No. 2, 2016, pp. 392–407. https://doi.org/10.2514/1.B35836.

[8] Petro, E., Bruno, A., Lozano, P., Perna, L. E., and Freeman, D., "Characterization of the TILE Electrospray Emitters," *AIAA Propulsion and Energy Forum*, Virtual Event, 2020. https://doi.org/10.2514/6.2020-3612.

[9] Ma, C., Bull, T., and Ryan, C. N., "Plume Composition Measurements of a High-Emission-Density Electrospray Thruster," *Journal of Propulsion and Power*, Vol. 37, No. 6, 2021, pp. 816–831. https://doi.org/10.2514/1.B37996.

[10] Courtney, D. G., Alvarez, N., and Demmons, N., "Electrospray Thrusters for Small Spacecraft Control: Pulsed and Steady State Operation," *Joint Propulsion Conference*, Cincinnati, USA, 2018. https://doi.org/10.2514/6.2018-4654.

[11] Evensen, G., *Data Assimilation: The Ensemble Kalman Filter*, 2nd ed., Springer Science & Business Media, 2009. https://doi.org/10.1007/978-3-642-03711-5.

[12] Guerra-Garcia, C., Krejci, D., and Lozano, P. C., "Spatial Uniformity of the Current Emitted by an Array of Passively Fed Electrospray Porous Emitters," *Journal of Physics D: Applied Physics*, Vol. 49, No. 11, 2016, p. 115503. https://doi.org/10.1088/0022-3727/49/11/115503.

[13] Courtney, D., Wood, Z., and Fedkiw, T., "Reconstructing Electrospray Plume Current Spatial Distributions using Computed Tomography," *36th International Electric Propulsion Conference*, University of Vienna, Austria, 2019.

[14] Chen, C., Chen, M., Fan, W., and Zhou, H., "Effects of Non-Uniform Operation of Emission Sites on Characteristics of a Porous Electrospray Thruster," *Acta Astronautica*, Vol. 178, 2021, pp. 192–202. https://doi.org/10.1016/j.actaastro.2020.09.002.

[15] Krejci, D., Mier-Hicks, F., Fucetola, C., Lozano, P., Hsu Schouten, A., and Martel, F., "Design and Characterization of a Scalable Ion Electrospray Propulsion System," *34th International Electric Propulsion Conference*, Hyogo-Kobe, Japan, 2015.

[16] Pettersson, G. M., Jia-Richards, O., and Lozano, P. C., "Development and Laboratory Testing of a CubeSat-Compatible Staged Ionic-Liquid Electrospray Propulsion System," *AIAA SciTech Forum*, San Diego, USA, 2022. https://doi.org/10.2514/6.2022-0040.

[17] Demmons, N. R., Wood, Z. D., Margousian, A., Knott, J., and Fedkiw, T., "Electrospray Attitude Control System Flight Preparation," *AIAA SciTech Forum*, San Diego, USA, 2022. https://doi.org/10.2514/6.2022-0039.

[18] Jia-Richards, O., Marzouk, Y. M., and Lozano, P. C., "On-Orbit Thrust Inference from Low-Acceleration Orbital Maneuvers via the Ensemble Kalman Update," In preparation.